CCS Chemistry

RESEARCH ARTICLE

Received: Nov. 19, 2019 | Accepted: Dec. 9, 2019

β-Cyclodextrin Decorated CdS Nanocrystals Boosting the Photocatalytic Conversion of Alcohols

Juan Wang[†], You-Xiang Feng[†], Min Zhang, Chao Zhang, Ming Li, Sheng-Jie Li, Wen Zhang* & Tong-Bu Lu*

Institute for New Energy Materials and Low Carbon Technologies, School of Materials Science and Engineering, Tianjin University of Technology, Tianjin 300384 (China)

*Corresponding authors: zhangwen@email.tjut.edu.cn; lutongbu@tjut.edu.cn; [†]J. Wang and Y.-X. Feng contributed equally to this work.

Cite this: *CCS Chem.* **2020**, *2*, 81–88

Regarding the utilization of semiconductor nanocrystals (NCs) in photocatalysis, the significant challenge is to eliminate the hindrance of decorated surface ligands on the photocarrier transport while maintaining their overall stability. Herein, we report a novel and stable catalyst comprising CdS NCs and surface-bound mono-(6-mercapto-6-deoxy)-β-cyclodextrin (HS-β-CD) molecules (denoted as CdS-CD), which could convert alcohols selectively into diols or aldehydes and H_2 under visible light irradiation, with 100% atom utilization, using an aqueous medium as a green solvent. The decorated β-CD ligands did not only confer a good stability of CdS-CD in water but also showed a high host–guest affinity to the alcohol species, thereby, guaranteeing a close vicinity of alcohol molecules at the surface of CdS NCs and minimizing the hindrance of surface ligands on the photocarrier transport. As a result, the CdS-CD displayed much improved photocatalytic activity for the conversion of alcohols in aqueous media, compared with those of CdS-BF_4 NCs.

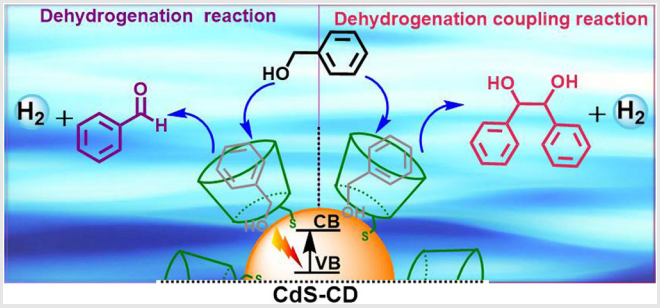

Keywords: CdS nanocrystals, β-cyclodextrin, alcohol, photocatalysis, dehydrogenative cross-coupling reactions

Introduction

The oxidation of alcohols into aldehydes or diols is a critical synthetic step in fragrance, confectionery, beverage, and pharmaceutical industries,[1–5] in which the conventional chemical oxidation of alcohols into aldehydes requires harsh conditions such as excess oxidants (CrO_3, IO_3^-, RuO_4, and MnO_2, and others), high temperature, high pressure, or organic medium. Such methods bring undesired side reactions, environmental problems, and waste of resources.[6–11] In this context, visible light–driven dehydrogenation of alcohols, which simultaneously generates valuable oxidation products and clean hydrogen is considered to be an ideal approach for the oxidation process due to its green feature and 100% atom utilization.[12–14]

DOI: 10.31635/ccschem.020.201900093
CCS Chem. **2020**, *2*, 81–88

Recently, semiconductor nanocrystals (NCs), especially, CdS NCs, have been demonstrated great promise in artificial photosynthesis.[15–23] Their significant extinction coefficients, tunable spectral range, and sufficient specific surface area features enable them to be superior light-absorber components of photocatalysts. However, linear organic ligands such as oleic acid are usually required to decorate the surface of the CdS NCs to achieve stable photocatalysts. Nonetheless, this strategy leads to a hindrance of the photocarrier transport,[22] as well as low solubility and stability in the aqueous medium. To increase the aqueous solubility of oleic acid–capped CdS NCs, Depalo et al[24,25] used α-cyclodextrin (α-CD) to form an inclusion complex between α-CD and oleic acid. They also used heptamine β-cyclodextrin to replace the octylamine molecules partially on the surface of CdS NCs in order to increase their aqueous solubility.[26] However, these modified CdS NCs are not good candidates for efficient photocatalysts, as the alkyl chain of oleic acid blocks the cavity of α-CD, and also, the existence of long linear organic chains around the surface of CdS NCs lead to a hindrance of the carrier transport. Therefore, developing an efficient and easy-to-prepare semiconductor NCs, which could balance stability and photogenerated carrier transport, along with efficient performance in aqueous media is highly desirable in photocatalysis.

Toward this goal, we were intrigued to mimic the function of an enzyme by decorating a mono-(6-mercapto-6-deoxy)-β-cyclodextrin (HS-β-CD) with hydrophobic cavity and hydrophilic outside surface[27–29] on the surface of CdS NCs (Scheme 1). We predicted that the introduction of HS-β-CD would exhibit the following advantages: (1) The S atom in HS-β-CD could strongly bind to the surface Cd(II) in CdS NCs to form stable CdS-CD composite in which the hydrophobic cavity of β-CD would selectively capture and enrich the organic reactants via host–guest interaction[30,31] at the surface of CdS NCs, and thus, minimize the hindrance of the carrier transport of the surface ligands on CdS NCs via close vicinity of the reactants with CdS NCs. (2) The outer hydrophilic surface of β-CD could generate high solubility and stability of CdS-CD in an aqueous medium like those found in cyclodextrins decorated metal nanoparticles.[32–34]

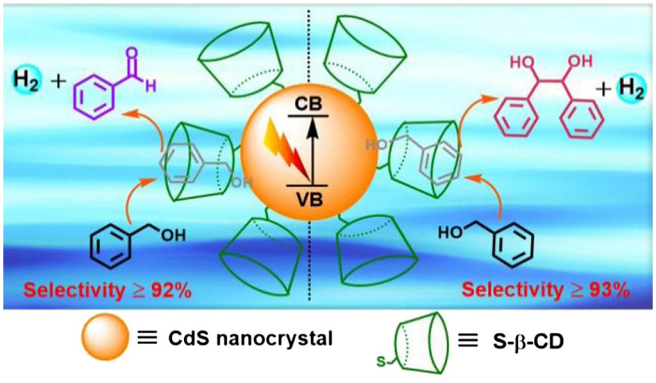

Scheme 1 | *Visible light–driven conversion of alcohols to H_2 and vicinal diols or aldehydes by β-CD-decorated CdS NCs.*

Motivated by our above assumptions, we synthesized a β-CD-decorated CdS NCs photocatalyst of CdS-CD and chose alcohol conversion as a model reaction to investigate the catalytic performance of photoredox reactions. As expected, the fabricated CdS-CD was able to convert efficiently, high and low concentrations of alcohol into vicinal diols and aldehydes, respectively, with up to 99% selectivity, accompanied by hydrogen emission. As far as we know, this is the first example of a metal-cocatalyst-free CdS NCs photocatalyst that could eliminate the hindrance associated with carrier transport of surface ligands, while maintaining the overall aqueous stability to achieve a highly selective and efficient conversion of alcohols in water into a variety and valuable organics.

Experimental Methods

Preparation of CdS-CD

HS-β-CD (70 mg) was dispersed in pure water by ultrasonication. Then methanol (5 mL) and chloroform (5 mL) were added, and the pH was adjusted to 11 with tetramethylammonium hydroxide (TMAOH). After that, CdS-OA in hexane solution (2 mL) was added to this mixture and stirred in the dark for 2 days. CdS-CD was precipitated with excess acetone and isolated by centrifugation (7000 rpm, 3 min). After washing with acetone, the CdS-CD was dispersed in water (1 mL).

Characterization of the fabricated CdS-CD NCs

To ensure that the modification of the CdS NCs surfaces had occurred, we characterized the fabricated complexes by proton nuclear magnetic resonance (^{1}H NMR), transmission electron microscopy (TEM), IR and UV–vis spectra, powder X-ray diffraction (XRD), and X-ray photoelectron spectroscopy (XPS) measurements (see supporting Figures S1–S8 for details).

Photocatalytic alcohol conversion into vicinal diols

Typically, a mixture of alcohol (0.3 M), CdS-CD (1 μM), and water (5 mL) were added into a quartz tube, and illuminated by a 450 nm light-emitting diode (LED) for 180 h at room temperature with continuous stirring, using a stirring bar. Products in the gas and liquid phases were identified by gas chromatography (GC) and gas chromatography–mass spectrometry (GC–MS; Agilent 7890B/5975B). Detailed GC–MS method is listed, as

DOI: 10.31635/ccschem.020.201900093
CCS Chem. **2020**, *2*, 81–88

follows: carrier gas: Helium; column (HP-5; length: 30 m, diameter: 0.25 mm, film: 0.25 μm), flow: 2.5 mL/min; front inlet temperature: 280 °C; flame ionization detector temperature: 300 °C; sample volume: 1 μL; split: 70:1; oven temperature: first kept at 60 °C for 3 min; and then increased to 280 °C at a rate of 15 °C/min. The alcohol conversion and selectivity were determined by high-performance liquid chromatography (HPLC). The species and selectivity of the products in the liquid phase were determined by GC–MS, HPLC, and column chromatography separation measurements.

Photocatalytic alcohol conversion into aldehyde

Typically, a mixture of alcohol (1 mM), CdS-CD (1 μM), and water (1 mL) were added into a quartz tube and illuminated by a 450 nm LED for 1.5 h at room temperature with continuous stirring, using a stirring bar. The species and selectivity of the liquid aldehyde products were determined by GC–MS and HPLC measurements by an external standard method.

More detailed experimental procedures and the characterization data are available as Supporting Information.

Results and Discussion

CdS-CD was prepared by ligand exchange of $^{-}$S-β-CD with oleic acid–capped CdS NCs (CdS-OA) (see Supporting Information). The results of ^{1}H NMR measurements indicate that all of the oleic acid anions on the surface of CdS NCs were replaced by $^{-}$S-β-CD (Supporting Information Figure S1), and the average numbers of $^{-}$S-β-CD on each

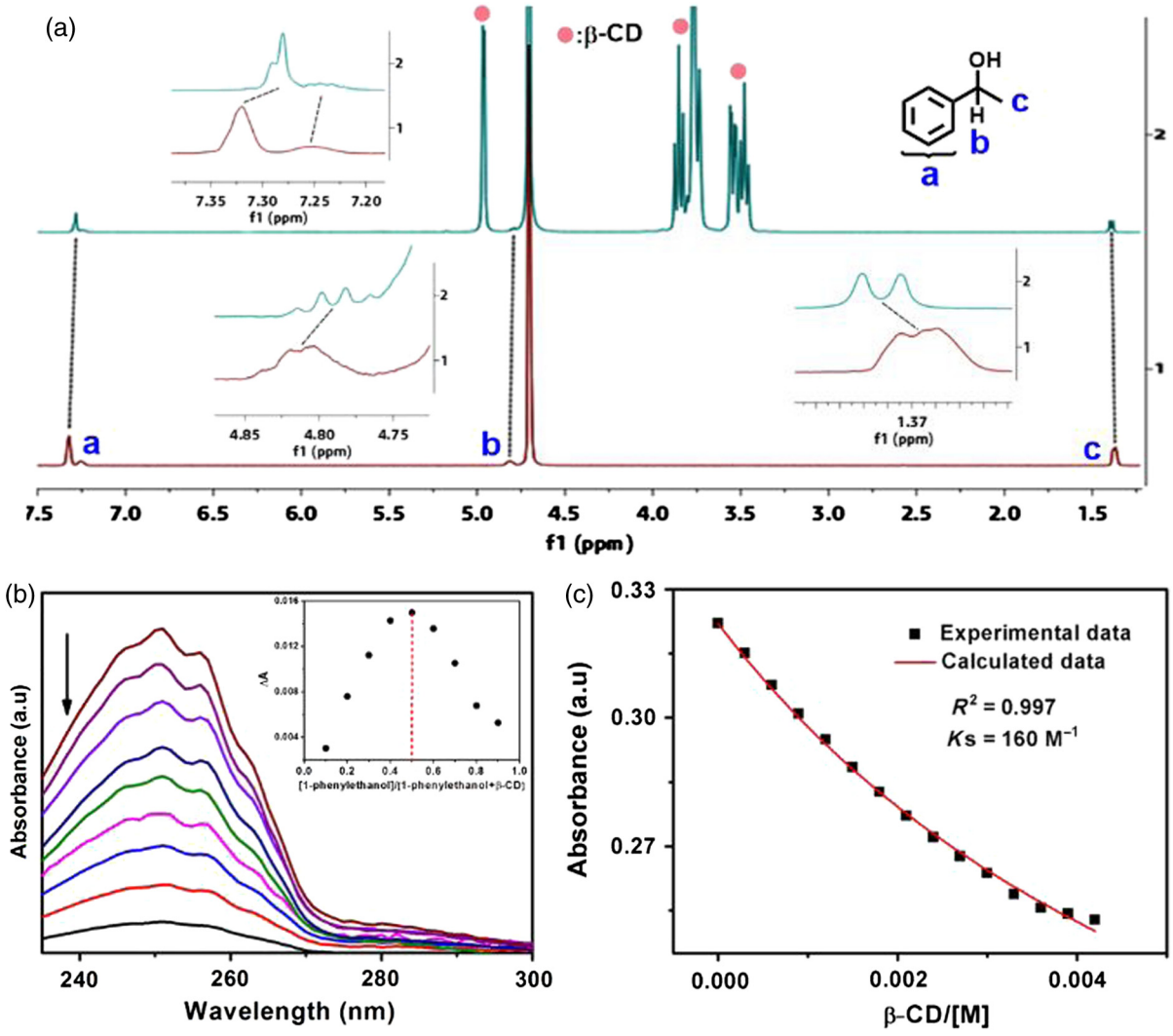

Figure 1 | *(a) Partial ^{1}H NMR spectra (400 MHz, D_2O, 25 °C) of 1-phenylethanol (red line) and 1-phenylethanol + β-CD (green line). (b) UV–Vis spectra of 1-phenylethanol ⊂ β-CD complex [(1-phenylethanol) + (β-CD) = 10.0 mM] at a different ratio. Inset: Job plot of 1-phenylethanol and β-CD. (c) The nonlinear least-squares analysis of the differential UV–vis spectral changes at 250 nm for the calculation of the Ks value for 1-phenylethanol ⊂ β-CD complex.*

DOI: 10.31635/ccschem.020.201900093
CCS Chem. **2020**, *2*, 81–88

CdS-CD was calculated to be 117 (Supporting Information Figure S2). The CdS-CD modification was validated by TEM, IR spectra, UV–vis spectra, powder X-ray diffraction (XRD), and XPS. The TEM image revealed that CdS-CD exists as uniform spherical nanoparticles, with an average size of 4.5 nm (Supporting Information Figure S3). The IR spectra showed three characteristic peaks around 3400, 2923, and 1032 cm^{-1} in both HS-β-CD and CdS-CD NCs (Supporting Information Figure S4), assigned to the O–H, C–H, and C–O stretching vibrations of $^{-}$S-β-CD backbone, respectively, while the UV–vis spectrum indicated that CdS-CD could absorb light below 490 nm (Supporting Information Figure S5). A powder XRD pattern showed that CdS-CD is a cubic phase structure (Supporting Information Figure S6). The XPS measurement indicates that the CdS-CD is mainly composed of Cd, S, C, and O elements (Supporting Information Figure S7). All the above results demonstrated the successful decoration of β-CD on the surface of CdS NCs. The results of the water solubility and stability test indicated that after β-CD decoration, CdS-CD could disperse well in water, and could be kept stable for more than 6 months, whereas CdS-OA NCs could not dissolve in water (Supporting Information Figure S8).

We identified the host–guest interactions between β-CD and the reactants in a photodehydrogenation reaction choosing 1-phenylethanol and benzyl alcohol as model substrates. For ^{1}H NMR measurements of 1-phenylethanol and 1-phenylethanol@β-CD, shown in Figure 1a, the protons of phenyl and methylene groups in 1-phenylethanol displayed an upfield shift, while those of methyl groups revealed a downfield shift, indicating that 1-phenylethanol was captured into the hydrophobic cavity of β-CD.[27] Furthermore, the complex stoichiometry between β-CD and 1-phenylethanol was measured to be 1:1 using Job's plot (Figure 1b, inset), indicating that only one 1-phenylethanol could be incorporated into the cavity of each β-CD. The binding constant (*K*s) between β-CD and 1-phenylethanol was determined as 160 M^{-1} (Figure 1c). Similar experiments were carried out on benzyl alcohol@β-CD (Supporting Information Figure S9) and 2-furanmethanol@β-CD (Supporting Information Figure S10). The results also indicated that benzyl alcohol and 2-furanmethanol could be encapsulated into the cavity of β-CD. Further, the ^{1}H–^{1}H ROESY spectra for benzyl alcohol@CdS-CD and 1-phenylethanol@CdS-CD inclusion complexes unveiled correlation peaks between the alcohols and β-CD (Supporting Information Figures S11 and S12), demonstrating the existence of noncovalent host–guest interactions between β-CD and alcohols.

To verify the photocatalytic performance toward dehydrogenation of alcohols in an aqueous medium, CdS-CD was employed as a sole photocatalyst. For comparison, CdS-BF_4 NCs (ligand-free NCs, previously demonstrated to show higher hydrogen production activity than water-soluble mercaptopropionic acid–capped CdS NCs[17]), were also prepared as a comparative photocatalyst. The time profile for the H_2 evolution was recorded to monitor the progress of the photoreaction. For the dehydrogenation of benzyl alcohol-catalyzed reaction by CdS-BF_4 NCs (Figure 2a, blue line, and Table 1, entry 1), the amount of H_2 liberated reached 5.4 μmol and stopped increasing, that is, reached saturation after 30 h. For the CdS-CD system (Figure 2a, black line), however, the H_2 liberation reached as high as 77 μmol after 180 h, which is 14.3 times higher than that of the prototype CdS-BF_4. The enhanced activity of CdS-CD could be attributable to the improved aqueous stability of CdS-CD, as well as an enrichment effect of the reactant at the surface of the CdS NCs through the host–guest interaction, which could consume the photogenerated carriers in a timely fashion. Indeed, when amantadine hydrochloride (And-HCl) was added to the

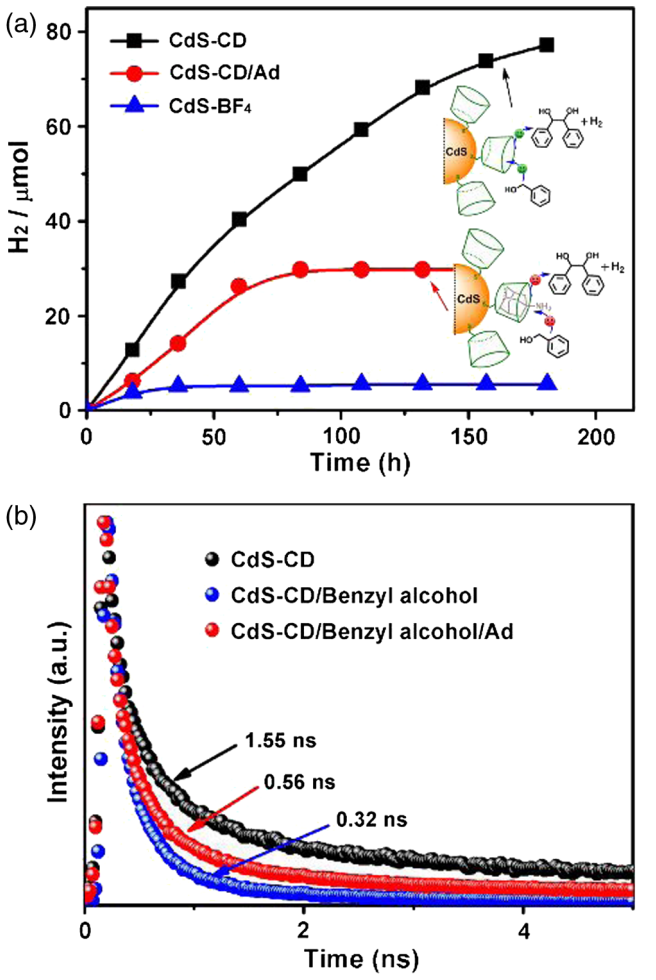

Figure 2 | *(a) Photocatalytic evolution of H_2 by CdS-CD (black), CdS-BF_4 (blue), and CdS-CD with adding 0.5 mM of amantadine (Ad, red). Reaction conditions: [CdS-CD] = [CdS-BF_4] = 1 μM, benzyl alcohol (0.3 M) in 5 mL H_2O, 450 nm LED light, 25 °C. (b) Photoluminescence decay of CdS-CD (black), CdS-CD/benzyl alcohol (blue), and CdS-CD/benzyl alcohol/Ad (red) detected at 519 nm.*

DOI: 10.31635/ccschem.020.201900093
CCS Chem. **2020**, *2*, 81–88

reaction system to block the cavity of β-CD partially, the amount of H_2 was dramatically decreased (Figure 2a, red line). Similar phenomenon was observed in 1-phenylethanol (Supporting Information Figure S13; and Table 1, entry 2) and 2-furanmethanol (Supporting Information Figure S14; and Table 1, entry 8) photocatalytic systems, demonstrating that both the photocatalytic activity and stability of CdS NCs could promote the decoration of β-CD on the surface of CdS NCs, and host–guest interactions play a key role for its high photocatalytic activity. To rule out the oxidation of the CD rings on the CdS NCs, a control experiment was set up without an addition of alcohol; the results indicated that CdS-CD, on its own, could not be oxidized to generate H_2 (Table 1, entry 10), thereby, verifying the stability of CdS-CD during the photocatalytic process.

For the liquid product in both CdS-CD and CdS-BF_4 reaction systems with various substituted phenyl and heteroaromatic benzyl alcohols (Table 1, entry 1–8; and Supporting Information Figure S15), bimolecular C–C coupling product of vicinal diols were the main products, along with trace amount of benzaldehydes and almost equivalent H_2 liberation. Notably, in any instance where the amount of the liberated H_2, was slightly less than that of the corresponding diol, we attributed the event to H_2 leakage during the photocatalytic process. The selectivity for vicinal diols was determined to be 93–99% by HPLC measurements (see Table 1). Table 1 shows that the amounts of diols in all CdS-CD systems were remarkably higher than those of CdS-BF_4 systems. Additionally, β-CD showed a steric hindrance effect on the catalytic activity

Table 1 | *The Visible Light–Driven Photocatalytic Results of Various Alcohols*

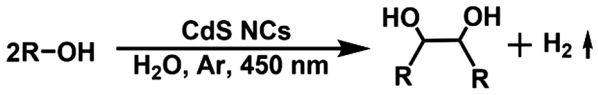

Entry	R–OH	Selectivity (%)	CdS-CD		CdS-BF_4	
			n H_2 (μmol)	n Diol (μmol)	n H_2 (μmol)	n Diol (μmol)
1	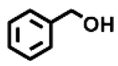	99	77.1	84.8	5.4	6.0
2		93	145.6	159.1	30.3	30.7
3	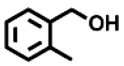	99	14.2	15.8	1.0	1.1
4	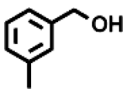	99	51.1	57.2	12.9	13.5
5	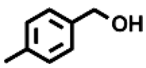	99	49.8	55.8	8.8	9.1
6	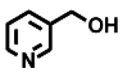	99	43.8	49.9	5.3	6.0
7	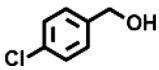	96	48.4	55.7	4.0	4.5
8	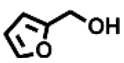	97	14.8	17.0	1.5	1.7
9	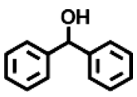	–	1.6	–	–	–
10	–	–	0	0	–	–

Reaction conditions: [CdS-CD] = [CdS-BF_4] = 1 μM, alcohol (0.3 M) in 5 mL H_2O, reaction time 180 h. 450 nm LED light at 25 °C. The horizontal line means the product yield was too little to allow detection.

DOI: 10.31635/ccschem.020.201900093
CCS Chem. **2020**, *2*, 81–88

of three methylbenzyl alcohol isomers (Table 1, entry 3–5), in which 2-methylbenzyl alcohol showed much lower activity than 3- and 4-methylbenzyl alcohol. The steric hindrance effect was also observed for the conversion of an alcohol-bearing bulky group (Table 1, entry 9), further demonstrating that the host–guest interactions played a vital role during the photocatalytic reactions.

To further understand the role of β-CD on the enhancement of the photocatalytic activity of CdS NCs, the photocatalytic performance for γ-CD- and thioglycerol-decorated CdS NCs, namely, CdS-γCD and CdS-GL, as well as a mixture of CdS-BF_4 with the native β-CD (CdS-BF_4/β-CD) were investigated by utilizing each in the conversion of 1-phenylethanol to diols and H_2. As shown in Supporting Information Figure S16, the concentration of the liberated H_2 (121.5 μmol) of the CdS-γCD catalyzed reaction was slightly less than that of the CdS-CD catalyzed reaction (145.6 μmol), probably due to the weaker host–guest interaction caused by the larger cavity of γ-CD. Besides, the amounts of H_2 liberated in the reaction catalyzed by CdS-GL, CdS-BF_4/β-CD, and CdS-BF_4 were all much lower than that of CdS-CD (Supporting Information Figure S16), demonstrating the direct tethering of $^{-}$S-β-CD on the surface of CdS NCs, and the strong host–guest interaction between β-CD and the reactants, which were the main factors that rendered it with the outstanding photocatalytic performance.

As the intermolecular coupling reactions had a close relationship with the reactant concentrations, it prompted us to investigate the photocatalytic reaction of the CdS-CD system at varying alcohol concentrations. The results in Supporting Information Figure S17 show that as the concentration of benzyl alcohol decreased from 300 mM to 1 mM, the main product in the liquid solution gradually changed from vicinal diol to benzaldehyde. Specifically, with a fixed alcohol concentration of 1 mM (Figure 3), nearly 100% conversions (Figure 3, black bar) were achieved, with 92–98% selectivity for the aldehyde products (Figure 3, black dot). In striking contrast, for the CdS-BF_4 photocatalytic system, only 33–79% alcohol conversions (Figure 3, red bar) with 21–82% aldehyde selectivity (Figure 3, red dot) were obtained. These results further demonstrated that the host–guest interactions between β-CD and the reactant could simultaneously enhance the photocatalytic activity and selectivity of CdS NCs.

We explored the mechanism of the photoreaction of the modified CdS NCs by photoluminescence spectra measurements. In Figure 2b, we show that the addition of benzyl alcohol decreased the emission lifetime of CdS-CD from 1.55 to 0.32 ns, indicating that this carrier was transported efficiently from CdS-CD to benzyl alcohol. Moreover, the addition of Ad-HCl partially extended the lifetime of CdS-CD from 0.32 to 0.56 ns (Figure 2b, red line), indicating that the competitive bonding between Ad and the benzyl alcohol with β-CD likely hindered the carrier transfer from CdS-CD to benzyl alcohol. These results undoubtedly demonstrate that the hindrance of the carrier transport could be eliminated effectively through tethering of $^{-}$S-β-CD on the surface of CdS NCs, as the captured reactants made contact directly to the surface of CdS NCs. The electron paramagnetic resonance (EPR) of the solution of benzyl alcohol@CdS-CD was also measured, using 5,5-dimethyl-1-pyrroline-N-oxide (DMPO) as a radical trap. As shown in Scheme 2 (inset), with light irradiation, the characteristic EPR signals of alkyl carbon radical and DMPO adducts (a_N = 15.0 G, a_H = 21.8 G) was detected, suggesting the

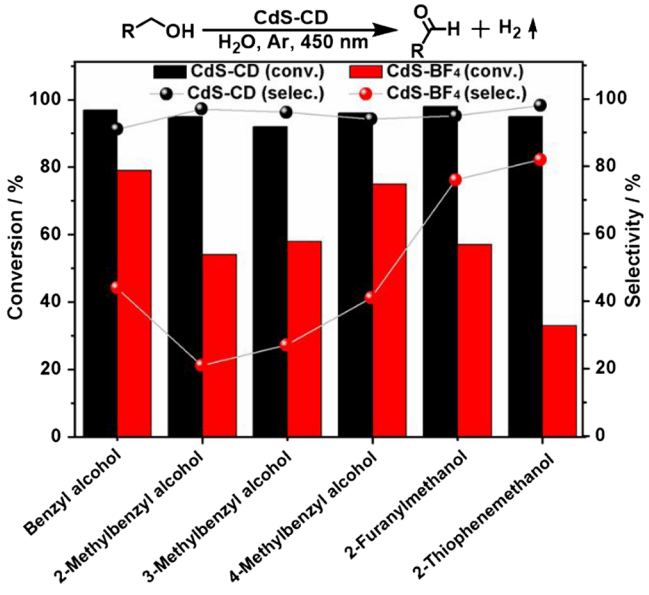

Figure 3 | *The results of comparative experiments for the photocatalytic reaction of CdS-CD and CdS-BF_4. Reaction conditions: [CdS-CD] = [CdS-BF_4] = 1 μM, benzyl alcohol(1 mM) in 1 mL H_2O, reaction time 1.5 h, 450 nm LED light, 25 °C.*

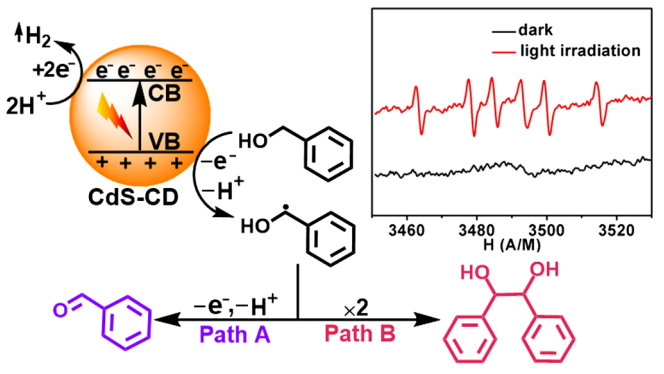

Scheme 2 | *The proposed photocatalytic mechanism for the benzyl alcohol@CdS-CD system (inset: EPR data).*

DOI: 10.31635/ccschem.020.201900093
CCS Chem. **2020**, *2*, 81–88

generation of benzyl radicals during the photocatalytic process.[35] Also, the kinetic isotope effect (KIE) was investigated using 4-methylbenzyl alcohol and deuterated 4-methylbenzyl alcohol as the reactants to confirm the hydrogen abstraction process (Supporting Information Table S1). The ratio of the reaction rates (k_H/k_D) was measured to be 4.4, indicating that the activation of the C–H bond at the benzylic position was involved in the rate-determining step.

Collectively, based on our results, we proposed a photocatalytic mechanism for the conversion of alcohols using benzyl alcohol as a model reaction presented in Scheme 2. Initially, under visible light irradiation, photoexcited electron and hole were generated in CdS-CD. Owing to the host–guest interaction, benzyl alcohol could be introduced into the cavity of the β-CD and approach the surface of CdS. Thus, the photogenerated hole on the surface of the CdS-CD could abstract one electron readily from the benzylic position to generate a benzyl radical after deprotonation. The benzyl radical might go through two different pathways, as follows: Under higher alcohol concentration, two benzyl alcohol radicals could go through a C–C coupling reaction to form a vicinal diol (Path B). At lower alcohol concentration, the benzyl radical would continue to be oxidized by the photogenerated holes in CdS-CD to form an aldehyde (Path A). At the same time, the protons in aqueous solution could be reduced to hydrogen by the photogenerated electrons in CdS-CD. The overall photoreaction process only needs visible light energy input; besides, it could be conducted in water, which is energy-efficient and environment-friendly, with the generation of highly valuable products and 100% atom utilization.

Conclusions

We have synthesized β-CD-decorated CdS NCs via a ligand-exchange reaction between $^{-}$S-β-CD- and oleic-acid-protected CdS NCs, which could be used as a robust and efficient photocatalyst for the conversion of alcohols into diols or aldehydes, with the liberation of H_2 in aqueous medium under visible light irradiations. Benefiting from the host–guest interaction between β-CD and the reactants, CdS-CD showed much superior activity and selectivity than those of CD-free CdS NCs (CdS-BF_4). Furthermore, tethering of $^{-}$S-β-CD on the surface of CdS NCs could also minimize the hindrance of carrier transport caused by surface ligands, as the captured reactants were more closely in contact with the surface of CdS NCs, and thus, the modified CdS-CD could also display higher photocatalytic activity than thioglycerol-decorated CdS NCs (CdS-GL). Our study provided a precise surface engineering strategy of semiconductor NCs for their photocatalytic applications in the oxidation of alcohols into uniquely valuable products through a green synthetic route with 100% atom utilization.

Supporting Information

Supporting Information is available.

Conflict of Interest

The authors declare no conflict of interest.

Acknowledgments

This work was supported financially by the National Key R&D Program of China (2017YFA0700104), NSFC (21702146, 21790052, and 21931007), and 111 Project of China (D17003). We thank Hong-Cai Zhou at Texas A&M University for assistance with corrections.

References

1. Mallat, T.; Baiker, A. Oxidation of Alcohols with Molecular Oxygen on Solid Catalysts. *Chem. Rev.* **2004**, *104*, 3037–3058.
2. Caron, S.; Dugger, R. W.; Ruggeri, S. G.; Ragan, J. A.; Ripin, D. H. B. Large-Scale Oxidations in the Pharmaceutical Industry. *Chem. Rev.* **2006**, *106*, 2943–2989.
3. Dincer, I. Green Methods for Hydrogen Production. *Int. J. Hydrogen Energy* **2012**, *37*, 1954–1971.
4. Balaraman, E.; Khaskin, E.; Leitus, G.; Milstein, D. Catalytic Transformation of Alcohols to Carboxylic Acid Salts and H_2 Using Water as the Oxygen Atom Source. *Nat. Chem.* **2013**, *5*, 122–125.
5. Chen, B.; Wu, L. Z.; Tung, C. H. Photocatalytic Activation of Less Reactive Bonds and Their Functionalization Via Hydrogen-Evolution Cross-Couplings. *Acc. Chem. Res.* **2018**, *51*, 2512–2523.
6. Gunanathan, C.; Milstein, D. Applications of Acceptorless Dehydrogenation and Related Transformations in Chemical Synthesis. *Science* **2013**, *341*, 1229712.
7. Uyanik, M.; Ishihara, K. Hypervalent Iodine-Mediated Oxidation of Alcohols. *Chem. Commun.* **2009**, *16*, 2086–2099.
8. Nielsen, M.; Alberico, E.; Baumann, W.; Drexler, H. J.; Junge, H.; Gladiali, S.; Beller, M. Low-Temperature Aqueous-Phase Methanol Dehydrogenation to Hydrogen and Carbon Dioxide. *Nature* **2013**, *495*, 85–89.
9. Johnson, T. C.; Morris, D. J.; Wills, M. Hydrogen Generation from Formic Acid and Alcohols Using Homogeneous Catalysts. *Chem. Soc. Rev.* **2010**, *39*, 81–88.
10. Fujita, K.; Kawahara, R.; Aikawa, T.; Yamaguchi, R. Hydrogen Production from a Methanol-Water Solution Catalyzed by an Anionic Iridium Complex Bearing a Functional Bipyridonate Ligand Under Weakly Basic Conditions. *Angew. Chem., Int. Ed.* **2015**, *54*, 9057–9060.
11. Nielsen, M.; Kammer, A.; Cozzula, D.; Junge, H.; Gladiali, S.; Beller, M. Efficient Hydrogen Production from Alcohols Under Mild Reaction Conditions. *Angew. Chem., Int. Ed.* **2011**, *50*, 9593–9597.

DOI: 10.31635/ccschem.020.201900093
CCS Chem. **2020**, *2*, 81–88

12. Zhao, L. M.; Meng, Q. Y.; Fan, X. B.; Ye, C.; Li, X. B.; Chen, B.; Wu, L. Z. Photocatalysis with Quantum Dots and Visible Light: Selective and Efficient Oxidation of Alcohols to Carbonyl Compounds Through a Radical Relay Process in Water. *Angew. Chem., Int. Ed.* **2017**, *56*, 3020–3024.
13. McClelland, K. P.; Weiss, E. A. Selective Photocatalytic Oxidation of Benzyl Alcohol to Benzaldehyde or C–C Coupled Products by Visible-Light-Absorbing Quantum Dots. *ACS Appl. Energy Mater.* **2018**, *2*, 92–96.
14. Chai, Z.; Zeng, T. T.; Li, Q.; Lu, L. Q.; Xiao, W. J.; Xu, D. Efficient Visible Light-Driven Splitting of Alcohols into Hydrogen and Corresponding Carbonyl Compounds over a Ni-Modified CdS Photocatalyst. *J. Am. Chem. Soc.* **2016**, *138*, 10128–10131.
15. Wu, L. Z.; Chen, B.; Li, Z. J.; Tung, C. H. Enhancement of the Efficiency of Photocatalytic Reduction of Protons to Hydrogen via Molecular Assembly. *Acc. Chem. Res.* **2014**, *47*, 2177–2185.
16. Li, X. B.; Gao, Y. J.; Wang, Y.; Zhan, F.; Zhang, X. Y.; Kong, Q. Y.; Zhao, N. J.; Guo, Q.; Wu, H. L.; Li, Z. J.; Tao, Y.; Zhang, J. P.; Chen, B.; Tung, C. H.; Wu, L. Z. Self-Assembled Framework Enhances Electronic Communication of Ultrasmall-Sized Nanoparticles for Exceptional Solar Hydrogen Evolution. *J. Am. Chem. Soc.* **2017**, *139*, 4789–4796.
17. Kuehnel, M. F.; Orchard, K. L.; Dalle, K. E.; Reisner, E. Selective Photocatalytic CO_2 Reduction in Water Through Anchoring of a Molecular Ni Catalyst on CdS Nanocrystals. *J. Am. Chem. Soc.* **2017**, *139*, 7217–7223.
18. Bi, Q.-Q.; Wang, J.-W.; Lv, J.-X.; Wang, J.; Zhang, W.; Lu, T.-B. Selective Photocatalytic CO_2 Reduction in Water by Electrostatic Assembly of CdS Nanocrystals with a Dinuclear Cobalt Catalyst. *ACS Catal.* **2018**, *8*, 11815–11821.
19. Lv, J. X.; Zhang, Z. M.; Wang, J.; Lu, X. L.; Zhang, W.; Lu, T. B. In Situ Synthesis of CdS/Graphdiyne Heterojunction for Enhanced Photocatalytic Activity of Hydrogen Production. *ACS Appl. Mater. Interfaces* **2019**, *11*, 2655–2661.
20. Yu, W. W.; Qu, L.; Guo, W.; Peng, X. Experimental Determination of the Extinction Coefficient of CdTe, CdSe, and CdS Nanocrystals. *Chem. Mater.* **2003**, *15*, 2854–2860.
21. Chang, C. M.; Orchard, K. L.; Martindale, B. C. M.; Reisner, E. Ligand Removal from CdS Quantum Dots for Enhanced Photocatalytic H_2 Generation in pH Neutral Water. *J. Mater. Chem.* **2016**, *4*, 2856–2862.
22. Harris, R. D.; Bettis Homan, S.; Kodaimati, M.; He, C.; Nepomnyashchii, A. B.; Swenson, N. K.; Lian, S.; Calzada, R.; Weiss, E. A. Electronic Processes Within Quantum Dot-Molecule Complexes. *Chem. Rev.* **2016**, *116*, 12865–12919.
23. Wu, L. Y.; Mu, Y. F.; Guo, X. X.; Zhang, W.; Zhang, Z. M.; Zhang, M.; Lu, T. B. Encapsulating Perovskite Quantum Dots in Iron-Based Metal–Organic Frameworks (MOFs) for Efficient Photocatalytic CO_2 Reduction. *Angew. Chem., Int. Ed.* **2019**, *58*, 9491–9495.
24. Depalo, N.; Comparelli, R.; Striccoli, M.; Curri, M. L.; Fini, P.; Giotta, L.; Agostiano, A. α-Cyclodextrin Functionalized CdS Nanocrystals for Fabrication of 2/3D Assemblies. *J. Phys. Chem. B* **2006**, *110*, 17388–17399.
25. Depalo, N.; Comparelli, R.; Curri, M. L.; Striccoli, M.; Agostiano, A. Cyclodextrin Mediated Phase Transfer in Water of Organic Capped CdS Nanocrystals. *Synth. Met.* **2005**, *148*, 43–46.
26. Depalo, N.; Comparelli, R.; Huskens, J.; Ludden, M. J.; Perl, A.; Agostiano, A.; Curri, M. L. Phase Transfer of CdS Nanocrystals Mediated by Heptamine β-Cyclodextrin. *Langmuir* **2012**, *28*, 8711–8720.
27. Zhang, W.; Chen, Y.; Yu, J.; Zhang, X. J.; Liu, Y. Photo/Chemo Dual-Controlled Reversible Morphological Conversion and Chiral Modulation of Supramolecular Nanohelixes with Nanosquares and Nanofibers. *Chem. Commun.* **2016**, *52*, 14274–14277.
28. Zhang, Y. M.; Zhang, N. Y.; Xiao, K.; Yu, Q.; Liu, Y. Photo-Controlled Reversible Microtubule Assembly Mediated by Paclitaxel-Modified Cyclodextrin. *Angew. Chem., Int. Ed.* **2018**, *57*, 8649–8653.
29. Zhang, Y. M.; Liu, Y. H.; Liu, Y. Cyclodextrin-Based Multistimuli-Responsive Supramolecular Assemblies and Their Biological Functions. *Adv. Mater.* **2019**, 1806158.
30. Zhang, Y. M.; Xu, X.; Yu, Q.; Yu, H. J.; Liu, Y. Drug Displacement Strategy for Treatment of Acute Liver Injury with Cyclodextrin-Liposome Nanoassembly. *iScience* **2019**, *15*, 223–233.
31. Li, J. J.; Zhang, H. Y.; Zhang, Y.; Zhou, W. L.; Liu, Y. Room-Temperature Phosphorescence and Reversible White Light Switch Based on a Cyclodextrin Polypseudorotaxane Xerogel. *Adv. Opt. Mater.* **2019**, *7*, 1900589.
32. Palanisamy, S., Kokulnathan, T., Chen, S. M., Velusamy, V., Ramaraj, S. K. Voltammetric Determination of Sudan I in Food Samples Based on Platinum Nanoparticles Decorated on Graphene-β-Cyclodextrin Modified Electrode. *J. Electroanal. Chem.* **2017**, *794*, 64–70.
33. Liu, J., Alvarez, J., Kaifer, A. E. Metal Nanoparticles with a Knack for Molecular Recognition. *Adv. Mater.* **2000**, *12*, 1381–1383.
34. Noël, S., Léger, B., Ponchel, A., Philippot, K., Denicourt-Nowicki, A., Roucoux, A., Monflier, E. Cyclodextrin-Based Systems for the Stabilization of Metallic (0) Nanoparticles and Their Versatile Applications in Catalysis. *Catal. Today* **2014**, *235*, 20–32.
35. Michail, K.; Siraki, A. G. Post-Trapping Derivatization of Radical-Derived EPR-Silent Adducts: Application to Free Radical Detection by HPLC/UV in Chemical, Biochemical, and Biological Systems and Comparison with EPR Spectroscopy. *Anal. Chem.* **2012**, *84*, 6739–6746.

DOI: 10.31635/ccschem.020.201900093
CCS Chem. **2020**, *2*, 81–88